INTL JOURNAL OF ELECTRONICS AND TELECOMMUNICATIONS, 2020, VOL. 66, NO. 2, PP. 389-394
Manuscript received February 1, 2020; revised April, 2020. DOI: 10.24425/ijet.2020.131890

MOVPE Technology of Fe-Compensated InP Layers for the Quantum Cascade Laser Applications

Mikołaj Badura

***Abstract*—Quantum cascade laser is one of the most sophisticated semiconductor devices. Its technology requires extremely high precision and layers quality. Device performance is limited by thermal extraction form laser core. One of solutions is to apply highly resistivity epitaxial material acting as insulating layer on top of the QCL. Present work describes consequent steps of elaboration of MOVPE technology of Fe-compensated InP layers for further applications in quantum cascade lasers.**

***Keywords*—MOVPE technology, optoelectronics, quantum cascade lasers, epitaxy**

I. Introduction

THE quantum cascade lasers belong to the novel family of semiconductor sources of coherent radiation [1]. QCLs are unipolar devices. Their principle of working is based on intersubband transitions [2]. Wavelength of emitted radiation results from laser design - thicknesses of particular layers. There are two main material systems of QCLs: GaAs- and InP-based. Arsenides based technology is well known and cheaper, but phosphides technology has few unique advantages. First of all, InGaAs/AlInAs/InP superlattice provides much bigger band offset discontinuity [3]. Moreover, InP based claddings have better thermal and optical properties due to bigger refractive index contrast. Finally, in case of phosphide based QCLs there is possibility to form buried heterostructures by applying high resistivity InP:Fe material what significantly improves heat extraction from the active region.

Quantum cascade laser is one of the most sophisticated semiconductor device. Core of the laser consists of hundreds, or even thousands, of sub-nanometer thin layers. Core is however sandwiched between two relatively thick claddings. Taking into account requirement of high precision of deposition of thin layers, molecular beam epitaxy (MBE) is the first choice epitaxial method. However, there is significant disadvantage of using phosphorus in MBE chamber due to safety and memory effect issues. One of the possible solutions is to apply hybrid technology by using metalorganic vapour phase epitaxy (MOVPE) to deposit thick claddings on MBE-grown laser core.

One of the biggest issues concerning quantum cascade lasers is heat extraction from its core. Commonly used insulators passivating surface of laser's ridge unfortunately have very low thermal conductivity coefficient (Table I). Thus, they inhibit heat extraction from the device and limit its efficiency. In order to improve performance of the laser, there is necessity to elaborate technology of material, which is highly resistive and has high thermal conductivity coefficient, to passivate surface of the laser ridge.

TABLE I
THERMAL PROPERTIES OF MATERIALS [4]-[6]

<table>
<tr><th>Material</th><th>Thermal conductivity (bulk) [W/mK]</th><th>Thermal conductivity incl. interface [W/mK]</th></tr>
<tr><td>SiO_2</td><td>1.4</td><td>0.2</td></tr>
<tr><td>Si_3N_4</td><td>20</td><td>~2.8</td></tr>
<tr><td>InP</td><td colspan="2">70</td></tr>
</table>

II. Objectives

The best material to cover surface of the laser should be epitaxially deposited and lattice-matched to elements of the device. In case of InP-based QCL, indium phosphide could be the best choice. Unfortunately, undoped InP exhibits conductive nature. However, small addition of Fe atoms should act as a deep level trap to catch any carriers in InP layer. The aim of present work is to elaborate MOVPE technology of high resistivity InP material compensated by Fe atoms. Investigated material should be compatible with deposited by hybride technology QCL structures.

III. Experimental Details

Epitaxial growth was performed using AIXTRON 3×2" CCS MOVPE system. The following material sources were used: TMIn for group III, 100% PH_3 for group V and CP_2Fe as a source of iron atoms. Using H_2 as the carrier gas, growth pressure and temperature were constant (100 mbar and 645°C, respectively). Applied growth rates were equal to 1.14 and 4.34 μm/h, while mole fraction ration of Cp_2Fe source to TMIn varied from 0 to $4{,}58\times10^{-4}$. Group V to III ratio was stabilized at the level of 133.

Two schemes of test structures were designed. First design concerns single InP layer containing Fe atoms (Fig. 1a) and undoped InP layer as the reference (Fig. 1b). Those samples were made for high Cp_2Fe flow and are dedicated for structural, optical and morphology investigations.

This work was co-financed by Wrocław University of Science and Technology statutory grants and by the Polish National Centre for Research and Development through projects PBS2/A3/15/2013 (PROFIT), TECHMAT-STRATEG1/347510/15/NCBR/2018 (SENSE).

Mikolaj Badura with Faculty of Microsystem Electronics and Photonics, Wrocław University of Science and Technology, Janiszewskiego 11/17, 50-372 Wrocław, Poland (e-mail: mikolaj.badura@pwr.edu.pl)

© The Author(s). This is an open-access article distributed under the terms of the Creative Commons Attribution License (CC BY 4.0, https://creativecommons.org/licenses/by/4.0/), which permits use, distribution, and reproduction in any medium, provided that the Article is properly cited.

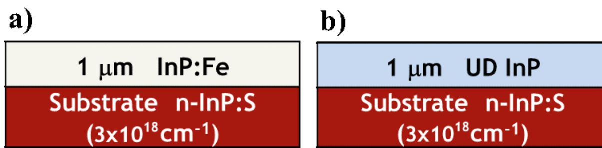

Fig. 1. Scheme of test samples containing Fe-compensated InP layer (a) and undoped InP reference (b).

Second scheme concerns cylindrical resistors with investigated layer capped between two pairs of InGaAs/InP undercontact layers. Applied InGaAs layers are lattice matched to InP and their purpose is to allow selective etching self-stopped at the beginning of particular layers. While top metal contact is placed at the center of structure, bottom one is placed around cylindrical resistor. In this case samples are also divided into Fe-compensated (Fig. 2a) and reference one (Fig. 2b). Those samples also were made for high Cp_2Fe flow and then quantity of Fe atoms was optimized to obtain the highest quality of deposited layers.

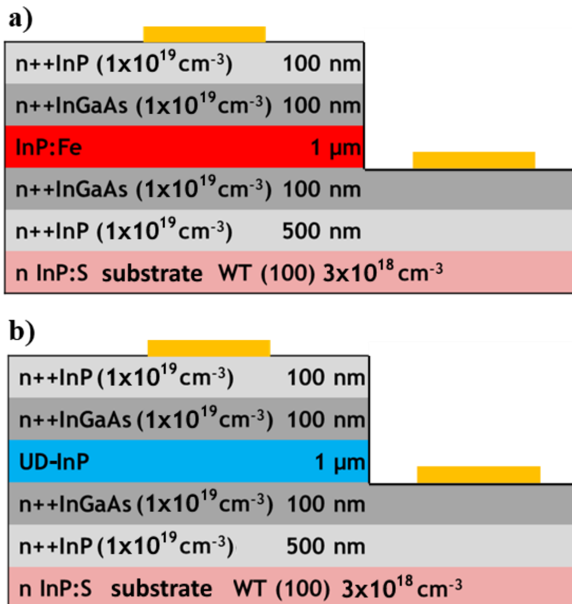

Fig 2. Scheme of structures for electrical measurements. Presented view is the cross-section of cylindrical resistors. Yellow rectangles stand for AuGe/Ni/Au metal contacts.

Prepared samples were measured by the means of high resolution X-Ray diffraction (HRXRD), photoluminescence, atomic force microscopy and 4-point current-voltage probe.

IV. RESULTS

The first aim was to investigate quality of deposited layers containing iron atoms as a comparison to reference samples. Crystalline quality of single layers was measured by the means of HRXRD. Diffractive curves around 004 peak are presented in Fig. 3. Results of Fe-compensated layer are compared with reference and substrate ones.

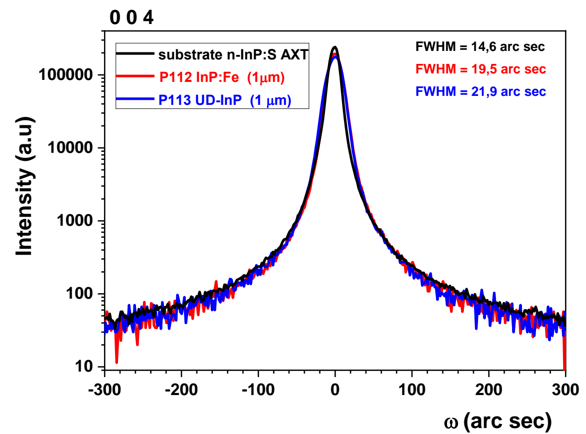

Fig. 3. High resolution X-Ray diffraction measurements of Fe-compensated InP layer in comparison with reference one and substrate.

Then morphology of deposited samples was observed by AFM (Fig. 4). As some disturbances of the surface were noticed in case of Fe-compensated sample, cross-section profile was also included (Fig. 4b).

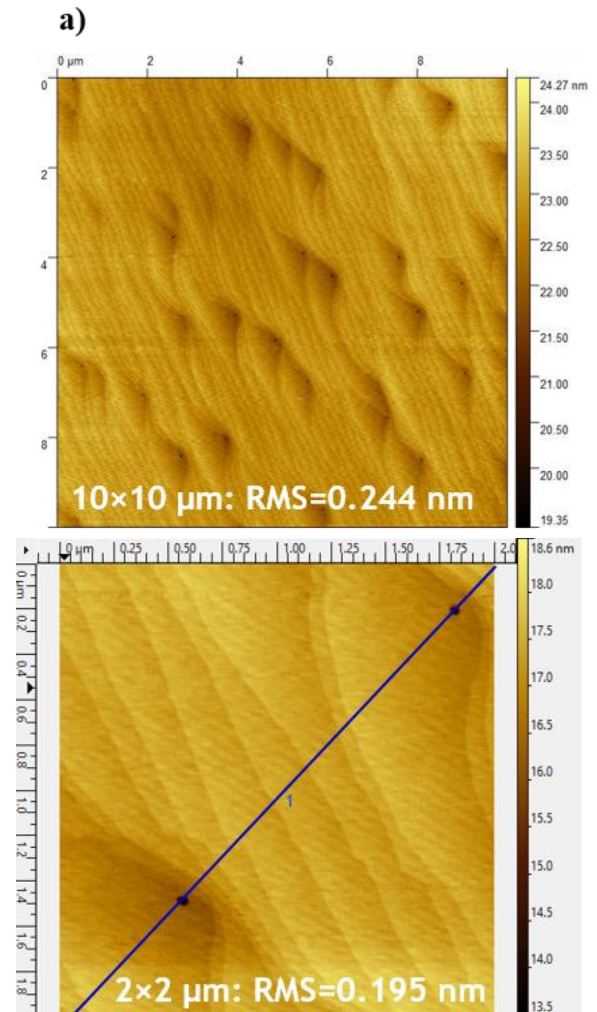

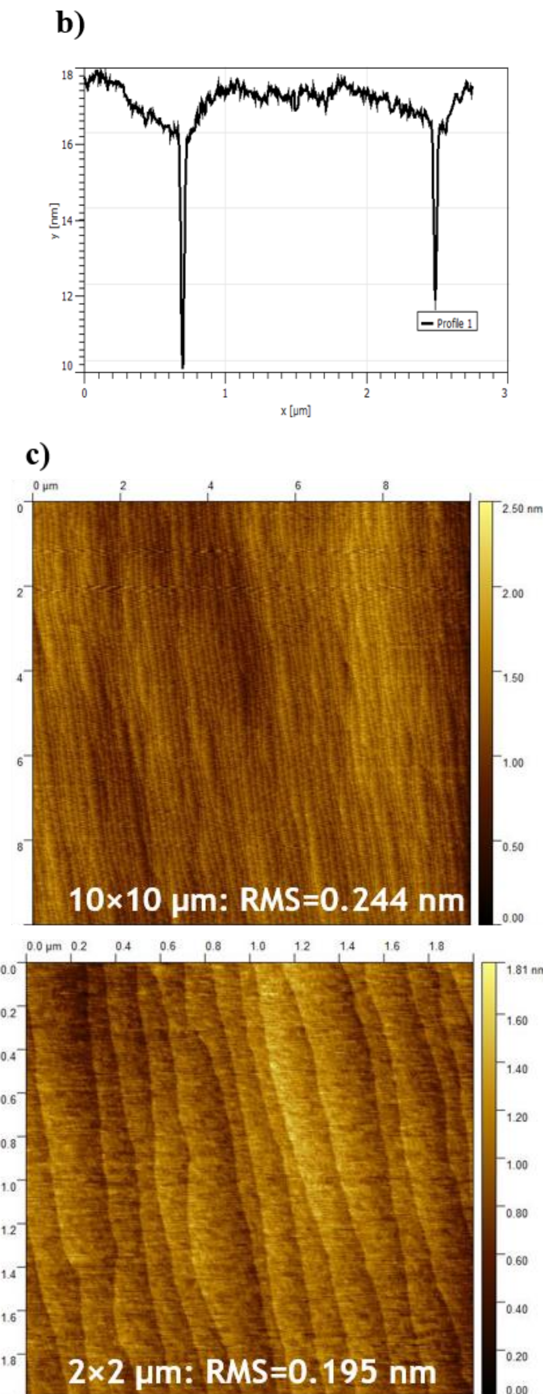

Fig. 4. Atomic force microscopy images of surface of Fe-compensated layer (a), its cross-section profile (b) and reference sample (c).

The influence of iron incorporation on optical quality of InP was investigated by photoluminescence spectroscopy. Low- and room-temperature spectra are shown in Fig. 5. Room-temperature spectrum of InP:Fe layer was multiplied by the factor of 10 due to weak response.

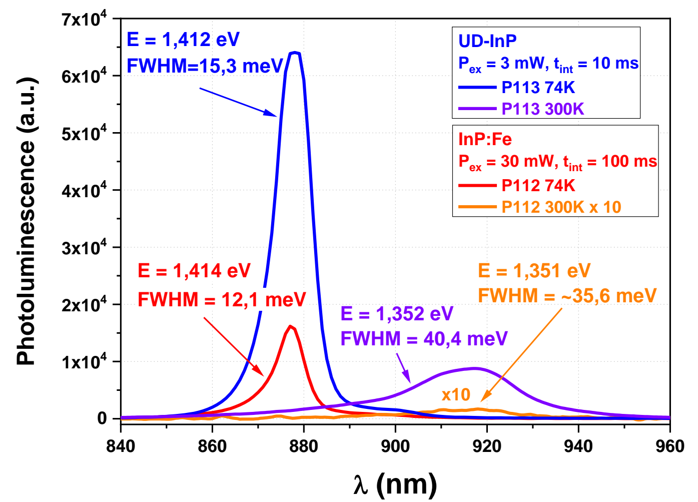

Fig. 5. Photoluminescence spectra of Fe-compensated InP layers (red and orange curves) and reference one (blue and violet ones), taken at room-temperature (right side) and 74K (left side).

Further steps concerns cylindrical resistors etched in investigated material. As those schemes are more complex, reciprocal space mapping analysis was made. Maps of the Fe-compensated sample and the reference are shown in Fig. 6.

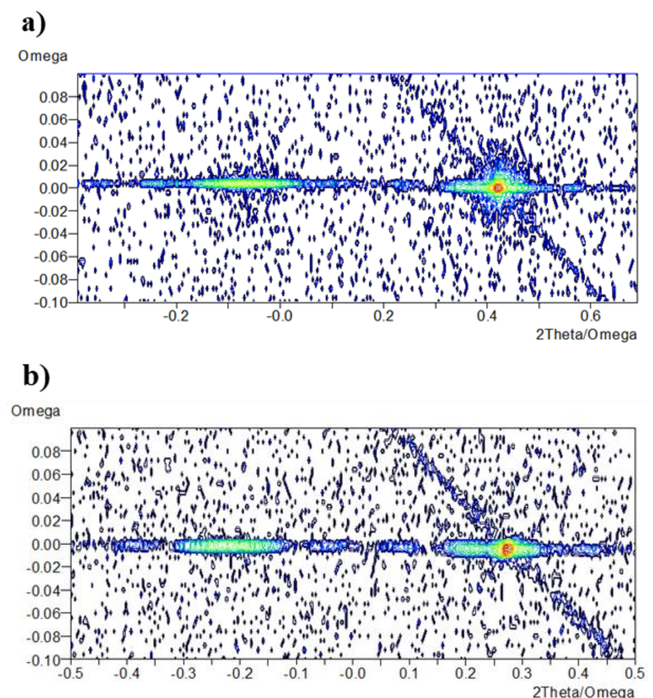

Fig. 6. XRD reciprocal space maps of epitaxial structure of cylindrical resistors for Fe-compensated InP layer (a) and undoped reference (b).

Influence of complex structure on its surface morphology is presented by AFM images in Fig. 7. In case of Fe-compensated structure there are still rich holes visible what is shown in Fig. 7c.

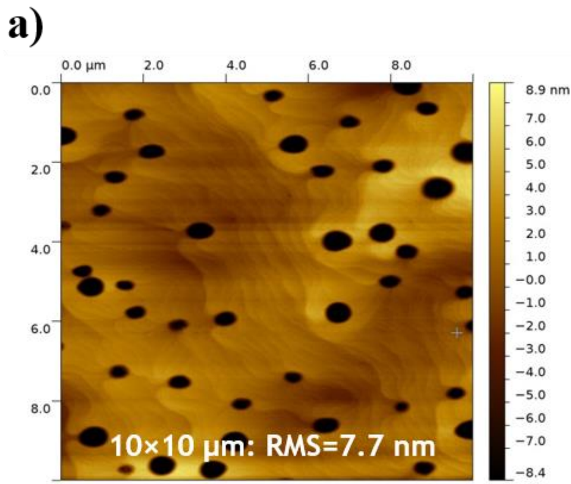

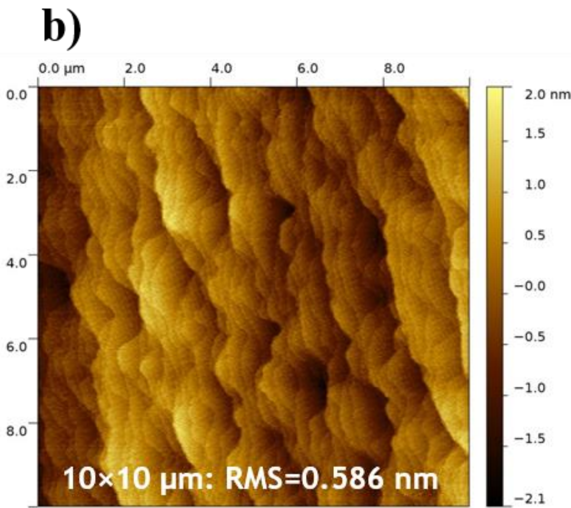

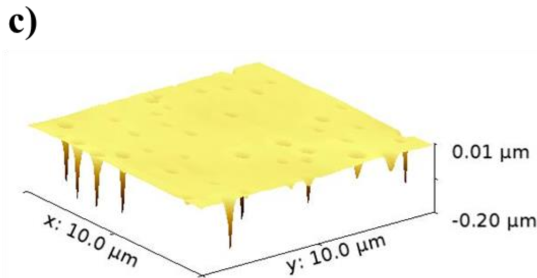

Fig. 7. AFM images of cylindrical structures including Fe-compensated (a) and undoped InP layers (b) together with 3D image of holes caused by Fe-rich regions (c).

From possible applications point of view, the most important are electric measurements. They were divided into two steps. Firstly, resistivity of metal contacts were investigated by TLM measurements. Current-voltage characteristics of top and bottom contacts are presented in Fig. 8.

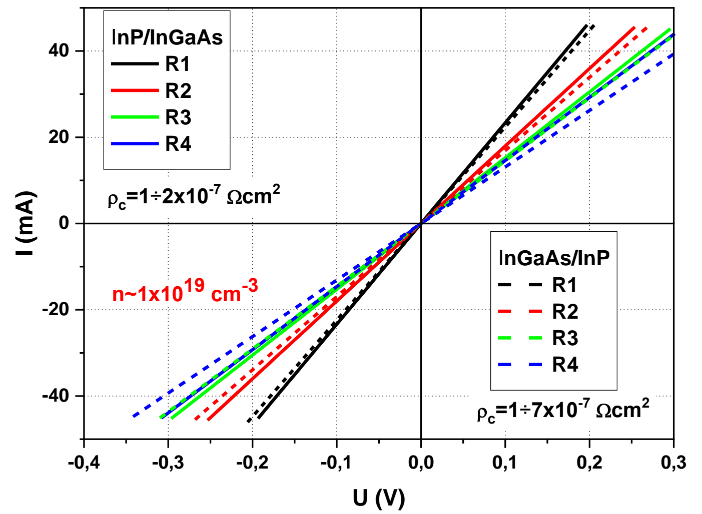

Fig. 8. Current-voltage characteristics of top (InP/InGaAs) and bottom (InGaAs/InP) metal contacts.

Then, resistance of resistors was measured, across the whole wafer. Exemplary characteristic and resistance distribution of different devices along wafer's diameter are presented in Fig. 9 for Fe-compensated devices and Fig. 10 for reference one.

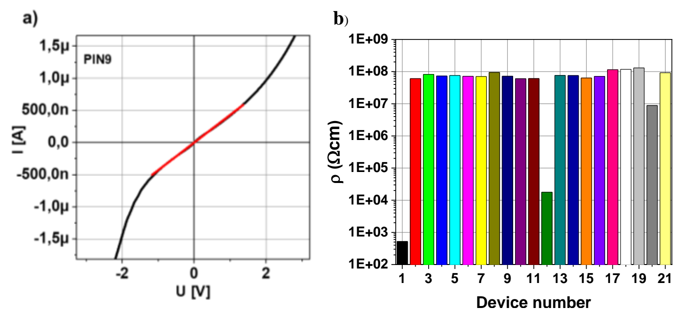

Fig. 9. I-V curve of exemplary cylindrical resistor and distribution of resistivity of investigated material across the whole wafer.

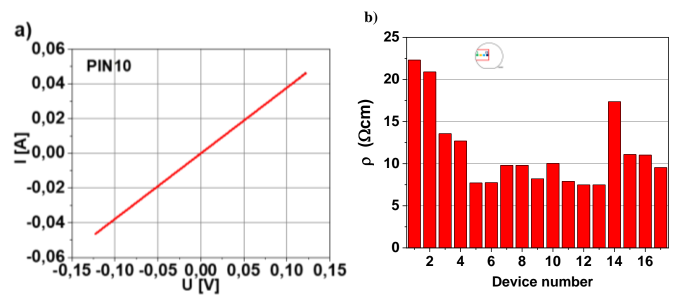

Fig. 10. I-V curve of exemplary reference resistor and distribution of resistivity of undoped InP material across the whole wafer.

V. DISCUSSION

Investigated material, as insulation part of the quantum cascade laser, should has high crystalline quality to avoid introduction of any disturbances into its structure. Thus HRXRD measurements were performed. Presented in Fig. 3. diffractive curves were measured for InP:Fe layers, as well as reference undoped InP and even for bare wafer. In case of investigated material, there are no visible any of additional peaks nor distortions, except of bulk InP one. Moreover, FWHM of every of those curves lies in range of 14.6÷21.9 arc sec, so are barely distinguishable. That facts indicate high crystalline quality and negligible impact of iron atoms.

However, when we look at AFM images in Fig. 4, we can see many deep holes on the InP:Fe surface. Those disturbances do not exist in case of the undoped reference. Such phenomenon is correlated with too much concentration of Fe atoms in the layer. According to [7], solubility limit of Fe can be described by following formula:

$$N_{Fe} = 3 \times 10^{21} \exp(-0.8 \pm 0.2\text{eV}/\,\text{kT}),$$

what means that at growth temperature of 645°C iron atoms will incorporate in crystal lattice only up to concentration of 1×10^{17} cm^{-3}. Above such limit excess atoms form iron droplets what cause growth disturbances, observed in Fig. 4. In case of reference sample, clear step-flow growth mode was observed.

Optical quality was verified by photoluminescence spectroscopy (Fig. 5). In case of room-temperature spectra, signal from InP:Fe layer is much weaker than reference one. In order to observe any changes, this signal was multiplied by factor of 10. Low-temperature spectra are sharp and narrow in both cases, Fe-compensated and reference. Any broadening of peaks are not observed, but again signal is weaker in case of InP:Fe layers. Such behavior may indicates high optical quality of epitaxial layer but iron droplets distract some part of radiation.

Next step was to prepare epitaxial structure presented in Fig. 2. Such complex multilayers were measured by the means of reciprocal space mapping what is presented in Fig. 6. In case of both samples, Fe-compensated and reference, there is noticeable lattice mismatch of InGaAs layers what should be optimized in further steps. In case of surrounding of InP peak there is slightly diffusive scattering observed for InP:Fe structure, but no additional peak broadening exists. Such results confirm high crystalline quality of all epitaxial structure.

Similar to previous samples, in that case also presence of Fe droplets is observed in Fig. 7. Despite the fact that there are different layers above Fe-rich one, growth disturbances propagate up to the surface.

Thanks to the double undercontact layers, made of InP/InGaAs layers, such structure can be selectively etched to form bottom contact. Undercontact layers are heavily n-type doped, up to 1×10^{19} cm^{-3}. Thanks to that their influence on devices resistance can be neglected. Metal contacts were made of AuGe/Ni/Au. Their resistivity is presented in Fig. 8. Both contacts are linear and has low resistivity at the level of 10^{-7} Ωcm^2. As dimensions of prepared resistors are well known, resistivity of investigated material could be easily calculated from device's resistance.

What is worth to notice, addition of Fe atoms to InP epitaxial layer has huge impact on its resistivity. Resistivity of InP:Fe reached level of 1×10^8 Ωcm (Fig. 9) what value is seven orders of magnitude higher than reference undoped InP (Fig. 10). Moreover, distribution over diameter of the waver is uniform.

Nevertheless, growth disturbances are unacceptable from laser applications point of view. Thus, next step of investigation was to optimize growth conditions to avoid Fe droplets. The best results could be obtained in surrounding of the Fe solubility limit in InP. At that point all of Fe atoms are electrically active, and there is lack of exceed atoms.

Set of next InP:Fe based resistors were prepared where molar ratio of Cp_2Fe/TMIn was decreased by the factor of 2, 4, 8 and 16. Influence of amount of the Fe source on layer resistivity is presented in Fig. 11.

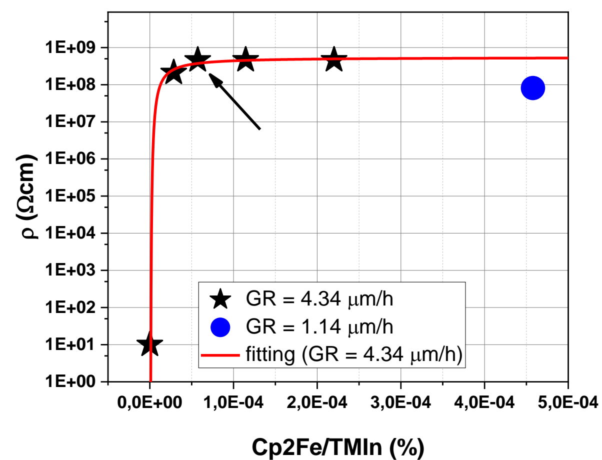

Fig. 11. Resistivity of the deposited InP:Fe material as a function of Cp2Fe/TMIn molar ratio.

The Fe solubility limit in InP is clearly visible in Fig. 11. Resistivity of marked sample has value of 4.6×10^8 Ωcm and further increasing of Fe amount does not change electrical properties. Such high resistivity fully meets the requirements of insulating layer for QCL applications. AFM images of sample grown at those conditions are presented in Fig. 12.

a)

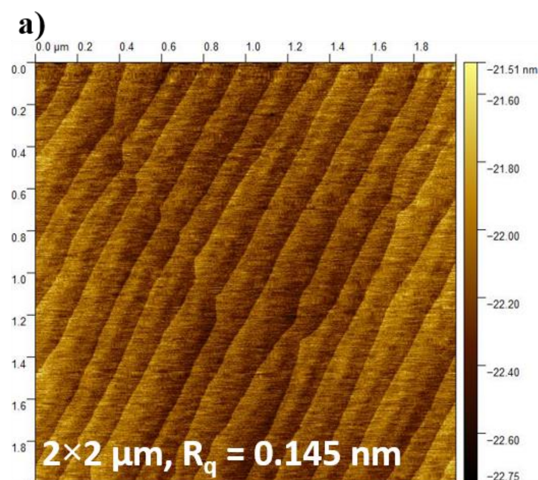

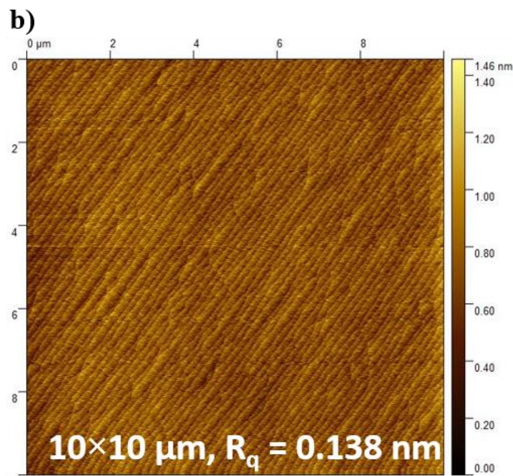

Fig. 12. AFM images of surface of InP:Fe layer deposited at optimal conditions. Roughness $R_q = 0.145$ nm.

At surface of that sample there are only sharp atomic edges visible, without any Fe correlated disturbances. With roughness as low as 0.1 nm and resistivity as high as 4.5×10^{8} Ωcm, material grown at that conditions is fully applicable to QCL technology.

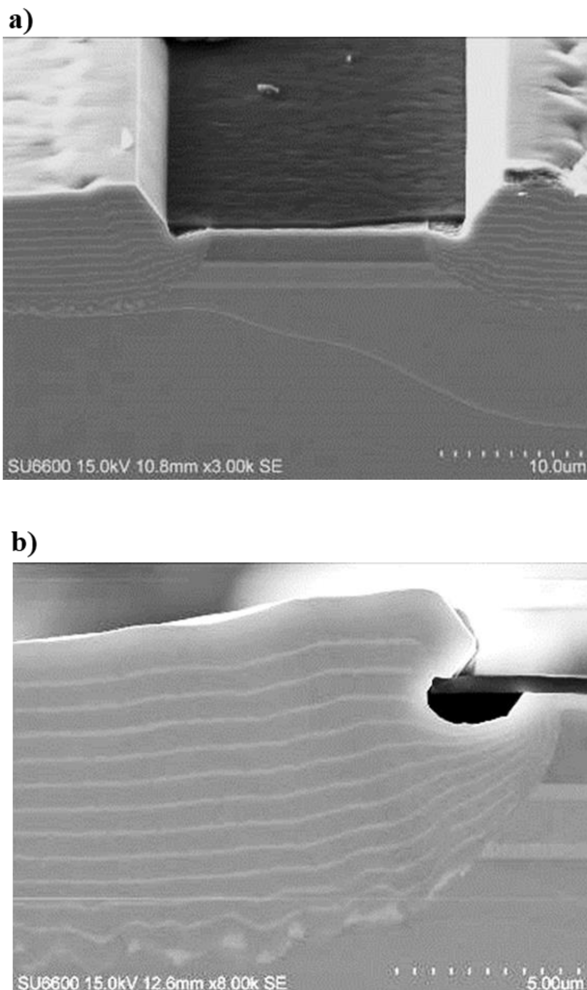

Fig 13. SEM images of elaborated InP:Fe layers deposited onto laser's ridge. Device was placed: parallel (a) and perpendicular to cut off (b).

Elaborated Fe-compensated InP layers were also deposited on already etched laser ridge. SEM images are presented in Fig. 13. Light lines are InGaAs markers to investigate growth rate as a function of the slope angle. It is visible that deposited layer perfectly covers edge of the ridge even in area which surface is much developed due to wet chemical etching. Thanks to that, such layer should ensure good heat extraction coefficient.

VI. Conclusions

Technology of quantum cascade lasers is demanding and challenging. Present work describes how MOVPE technology of highly resistive InP:Fe layers was elaborated for further application in QCL. It was noticed that growth conditions has to be optimized to obtain high crystalline, optical and morphology quality together with proper electrical properties. Best result were obtained for growth rate above 4 μm/h, process temperature T = 645°C and molar ratio $CP_2Fe/TMIn = 5.72\times10^{-5}$.

Further work concern investigation of influence of elaborated layers on device properties of QCL.

Acknowledgements

Author is very grateful to A. Szyszka for AFM and I. Sankowska for HRXRD measurements.

References

[1] C. Gmachl, F. Capasso, D.L. Sivco, A.Y. Cho, Recent progress in quantum cascade lasers and applications, Rep. Prog. Phys. 64 (2001) 1533–1601. doi:10.1088/0034-4885/64/11/204.

[2] J. Faist, F. Capasso, D.L. Sivco, C. Sirtori, A.L. Hutchinson, A.Y. Cho, Quantum Cascade Laser, Science (80-.). 264 (1994) 553–556. doi:10.1126/science.264.5158.553.

[3] M. Bugajski *et al*., Mid-IR quantum cascade lasers: Device technology and non-equilibrium Green's function modeling of electro-optical characteristics, Phys. Status Solidi. 251 (2014) 1144–1157. doi:10.1002/pssb.201350322.

[4] J. Jaramillo-Fernandez, E. Chavez-Angel, R. Sanatinia, H. Kataria, S. Anand, S. Lourdudoss, C.M. Sotomayor-Torres, Thermal conductivity of epitaxially grown InP: experiment and simulation, CrystEngComm. 19 (2017) 1879–1887. doi:10.1039/C6CE02642G.

[5] K.K. Ng, Complete Guide to Semiconductor Devices, John Wiley & Sons, Inc., Hoboken, NJ, USA, 2009. doi:10.1002/9781118014769.

[6] S.M. Sze, K.K. Ng, Physics of Semiconductor Devices, John Wiley & Sons, Inc., Hoboken, NJ, USA, 2006. doi:10.1002/0470068329.

[7] T. Takanohashi, K. Nakai, K. Nakajima, SIMS and DLTS measurements on Fe-doped InP epitaxial layers grown by MOCVD, *Jpn. J. Appl. Phys*. 27 (1988) L113–L115. doi:10.1143/JJAP.27.L113.